

DUAL SOLUTIONS ON BOUNDARY-LAYER FLOW OVER A MOVING SURFACE IN A FLOWING NANOFLUID WITH SECOND-ORDER SLIP

by

Najwa NAJIB^{a*}, Norfifah BACHOK^a, Norihan Md ARIFIN^a, and Ioan POP^b

^aDepartment of Mathematics and Institute for Mathematical Research,
Universiti Putra Malaysia, Selangor, Malaysia

^bDepartment of Applied Mathematics, Babes-Bolyai University, Cluj-Napoca, Romania

Original scientific paper
<https://doi.org/10.2298/TSCI180116205N>

The steady boundary-layer flow of a nanofluid past a moving semi-infinite flat plate in a uniform free stream in the presence of second order slip is studied using a second order slip flow model. The governing PDE are transformed into non-linear ODE by using appropriate similarity transformations, which are then solved numerically using bvp4c solver for different values of selected parameters. We found that the solutions existed for dual in a certain range of velocity ratio parameter. Therefore, a stability analysis has been analyzed to show which solutions are stable. The effects of velocity ratio parameter, Lewis number, Prandtl number, Brownian motion parameter, thermophoresis parameter, mass suction, first order slip parameter, and second order slip parameter on the skin friction coefficient, heat transfer coefficient, dimensionless velocity, temperature as well as nanoparticle volume fraction profiles are figured out graphically and discussed. These results reveals that the slip parameters expand the range of the solutions obtained. The increment of slip parameters lead to decrease the skin friction coefficient while increase the heat transfer coefficient. In addition, the value of Lewis number, Prandtl number, Brownian motion parameter, and thermophoresis parameter are significantly affected the heat transfer coefficient. Lastly, the first solution is stable and physically relevant, while the second solution is not.

Key words: *stability solution, moving surface, nanofluid, second-order slip, bvp4c, Brownian motion, thermophoresis, Lewis number, Prandtl number*

Introduction

The second order slip flow model was first introduced by Wu [1] and state that the improved slip model is derived from kinetic theory. Fang *et al.* [2] has used the proposed model [1] to solve the flow field past a shrinking sheet analytically. Then, Fang and Aziz [3] had extended the work into stretching sheet with presence of mass suction. Rosca and Pop [4] investigated the steady flow and heat transfer over a vertical permeable stretching/shrinking sheet and found that the characteristics of the flow are strongly influenced by the mixed convection, mass transfer and the slip flow model parameters. Rosca and Pop [5] studied the flow near stagnation point past a flat plate vertically with second order slip flow. Mabood and Das [6] discussed the slip effects on the boundary-layer flow of a nanofluid over a stretching sheet in the presence of

* Corresponding author, e-mail: najwamohdnajib@gmail.com

melting heat transfer and thermal radiation. The study on effect of mass transfer induced slip at a moving surface on gas-flows past a stretching/shrinking sheet was done by Wu [7]. Sharma and Ishak [8] considered the second order slip effects over a stretching sheet in Cu-water based nanofluid.

The multiple solutions (dual or more) of boundary-layer flow have been found in each study over past several years. The method of finding dual solutions and analyzing the stability of the solutions is importance in field of engineering, it is due to verify that which solution is a steady-state and physically relevant. Merkin [9] was among the first who made the analysis to test the stability flow. Then, Weidman *et al.* [10] considered the transpiration effects on boundary-layer flow over moving surfaces. Merrill *et al.* [11] investigated the mixed convection boundary-layer flow near stagnation point on a vertical surface embedded in a porous medium. Ishak [12] and Noor *et al.* [13] studied the stability analysis on the boundary-layer flow past a shrinking sheet in viscous fluid and nanofluid, respectively. Nazar *et al.* [14] has done the analysis on 3-D flow over a permeable shrinking surface in Cu-water nanofluid. Noor *et al.* [15] again considered the flow in nanofluid past a permeable moving plate. Hafidzuddin *et al.* [16] has done the work on unsteady 3-D viscous flow over a stretching/shrinking surface. Very recently, Yasin *et al.* [17] have implemented the stability analysis in their study on MHD flow with effects of viscous dissipation, Joule heating and partial velocity slip.

Apart from that, the problem of boundary-layer flow over a moving surface has been considered first by Blasius [18] in 1908. Klemp and Acrivos [19] studied the reverse flow over a moving wall. After that, Husaini *et al.* [20] proposed the same problems over a moving surface but under different observations. Fang [21, 22] discussed the similarity solutions on heat and mass transfer, respectively for a moving flat surface in boundary-layer flow. Again, Fang and Lee [23] presented and solved numerically a flow of a slightly rarefied gas over a moving surface. Hence, the purpose of this study is to extend the work by Bachok *et al.* [24] by using the second order slip flow modeled by Wu [1]. The numerical results obtained will be compared with the previous works. Some figures will be plotted and the characteristics of the flow will be discussed further. It is worth mentioning that no attempt has been made such present study.

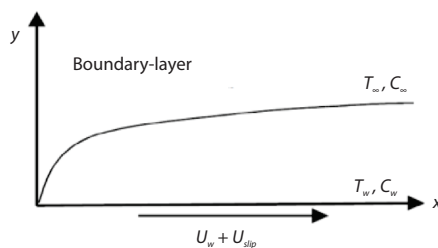


Figure 1. Physical model and co-ordinate system

the temperature, T , and the nanoparticle fraction, C , take constant values T_w and C_w , respectively, while the values of T and C in the ambient fluid (inviscid flow) are denoted by T_∞ and C_∞ , respectively. We consider a steady-state flow and make the standard boundary-layer approximations, based on a scale analysis, and write the governing eqs. (1)-(4) [25]:

$$\frac{\partial u}{\partial x} + \frac{\partial v}{\partial y} = 0 \quad (1)$$

Problem formulation

Consider the steady boundary-layer flow of a nanofluid past a moving semi-infinite flat plate in a uniform free stream as shown in fig. 1.

It is assumed that the velocity of the uniform free stream is U and that of the flat plate is $U_w = \lambda U$, where λ is the plate velocity parameter, see Weidman *et al.* [10]. The flow takes place at $y \geq 0$, where y is the co-ordinate measured normal to the moving surface. It is also assumed that at the moving surface,

$$u \frac{\partial u}{\partial x} + v \frac{\partial u}{\partial y} = \nu \frac{\partial^2 u}{\partial y^2} \quad (2)$$

$$u \frac{\partial T}{\partial x} + v \frac{\partial T}{\partial y} = \alpha \nabla^2 T + \Omega \left[D_B \frac{\partial C}{\partial y} \frac{\partial T}{\partial y} + \left(\frac{D_T}{T_\infty} \right) \left(\frac{\partial T}{\partial y} \right)^2 \right] \quad (3)$$

$$u \frac{\partial C}{\partial x} + v \frac{\partial C}{\partial y} = D_B \frac{\partial^2 C}{\partial y^2} + \left(\frac{D_T}{T_\infty} \right) \frac{\partial^2 T}{\partial y^2} \quad (4)$$

where u and v are the velocity components along the x - and y -axes, respectively, $\alpha = k/(\rho c)_f$ – the thermal diffusivity of the fluid, ν – the kinematic viscosity coefficient, and $\Omega = (\rho c)_p/(\rho c)_f$. Further, the coefficients that appear in eqs. (3) and (4) are the Brownian diffusion coefficient, D_B , and the thermophoretic diffusion coefficient, D_T . By using the revised boundary conditions proposed by Kuznetsov and Nield [26], eqs. (1)-(4) are subjected to the boundary condition:

$$u = \lambda U + U_{\text{slip}}, \quad v = v_w, \quad T = T_w, \quad D_B \frac{\partial C}{\partial y} + \frac{D_T}{T_\infty} \frac{\partial T}{\partial y} = 0 \quad \text{at } y = 0 \quad (5)$$

$$u \rightarrow U, \quad T \rightarrow T_\infty, \quad C \rightarrow C_\infty \quad \text{as } y \rightarrow \infty$$

where U_{slip} is defined:

$$U_{\text{slip}} = \frac{2}{3} \left(\frac{3 - \chi l^3}{\chi} - \frac{3}{2} \frac{1 - l^2}{\text{Kn}} \right) \omega \frac{\partial u}{\partial y} - \frac{1}{4} \left[l^4 + \frac{2}{\text{Kn}^2} (1 - l^2) \right] \omega^2 \frac{\partial^2 u}{\partial y^2} = A \frac{\partial u}{\partial y} + B \frac{\partial^2 u}{\partial y^2} \quad (6)$$

where A and B are constants, Kn is Knudsen number, $l = \min(1/\text{Kn}, 1)$, χ – the momentum accommodation coefficient with $0 \leq \chi \leq 1$, and ω – the molecular mean free path. Based on the definition of l , it is seen that for any given value of Knudsen number, we have $0 \leq l \leq 1$. Since the molecular mean free path ω is always positive it results in that B – the negative number.

The mathematical analysis of the problem is simplified by introducing the following dimensionless co-ordinates:

$$\psi = (2U\nu x)^{1/2} f(\eta), \quad \eta = (U/2\nu x)^{1/2} y, \quad \theta(\eta) = \frac{T - T_\infty}{T_w - T_\infty}, \quad \phi(\eta) = \frac{C - C_\infty}{C_w - C_\infty} \quad (7)$$

where ψ is the stream function defined as $u = \partial\psi/\partial y$ and $v = \partial\psi/\partial x$, which identically satisfies eq. (1). Substitute eq. (7) into eqs. (2)-(4), we obtain the following non-linear ODE:

$$f''' + f f'' = 0 \quad (8)$$

$$\frac{1}{\text{Pr}} \theta'' + f \theta' + \text{Nb} \phi' \theta' + \text{Nt} \theta'^2 = 0 \quad (9)$$

$$\phi'' + \text{Le} f \phi' + \frac{\text{Nt}}{\text{Nb}} \theta'' = 0 \quad (10)$$

and the boundary conditions eq. (9) becomes:

$$f(0) = s, \quad f'(0) = \lambda + \sigma f''(0) + \delta f'''(0), \quad \theta(0) = 1, \quad \text{Nb} \phi'(0) + \text{Nt} \theta'(0) = 0 \quad (11)$$

$$f'(\eta) \rightarrow 1, \quad \theta(\eta) \rightarrow 0, \quad \phi(\eta) \rightarrow 0 \quad \text{as } \eta \rightarrow \infty$$

We take:

$$v_w = -\frac{1}{2} \sqrt{\frac{2U\nu}{x}} f_0$$

where $f(0) = f_0 = s$ is a non-dimensional constant which determines the transpiration rate, with $s > 0$ for suction. In the aforementioned equations, primes denote differentiation with respect to η and the four parameters are defined:

$$\text{Pr} = \frac{\nu}{\alpha}, \quad Nb = \frac{(\rho C)_p D_B (C_w - C_\infty)}{(\rho C)_f \nu}, \quad \text{Le} = \frac{\nu}{D_B}, \quad Nt = \frac{(\rho C)_p D_T (T_w - T_\infty)}{(\rho C)_f T_\infty \nu} \quad (12)$$

where Pr is the Prandtl number, Le – the Lewis number, Nb – the Brownian motion parameter, and Nt – the thermophoresis parameter. Following Mukhopadhyay and Andersson [27], we take $A = (2x\nu/U)^{1/2}\sigma$ and $B = (2\nu x/U)\delta$ with $\sigma > 0$ being the first velocity slip and $\delta < 0$ is the second velocity slip parameters, see Fang *et al.* [2]. It is worth mentioning that the moving parameter $\lambda > 0$ corresponds to downstream movement of the plate from the origin, while $\lambda < 0$ corresponds to the upstream movement of the plate from the origin.

The physical quantities of interest are the skin friction coefficient, C_f , the local Nusselt number, and the local Sherwood number which are defined:

$$C_f = \frac{\tau_w}{\rho U^2}, \quad \text{Nu}_x = \frac{xq_w}{k(T_w - T_\infty)}, \quad \text{Sh}_x = \frac{xq_m}{D_B(C_w - C_\infty)} \quad (13)$$

where the wall shear stress τ_w , the local heat flux q_w , and the local mass flux q_m are given:

$$\tau_w = \mu \left(\frac{\partial u}{\partial y} \right)_{y=0}, \quad q_w = -k \left(\frac{\partial T}{\partial y} \right)_{y=0}, \quad q_m = -D_B \left(\frac{\partial C}{\partial y} \right)_{y=0} \quad (14)$$

with μ and k being the dynamic viscosity and thermal conductivity of the nanofluids, respectively. By using the similarity variables eq. (11), we obtain:

$$(2\text{Re}_x)^{1/2} C_f = f''(0), \quad \left(\frac{\text{Re}_x}{2} \right)^{-1/2} \text{Nu}_x = -\theta'(0), \quad \left(\frac{\text{Re}_x}{2} \right)^{-1/2} \text{Sh}_x = -\phi'(0) \quad (15)$$

where $\text{Re}_x = Ux/\nu$ is the local Reynolds number. In the present context, $\text{Re}_x^{-1/2} \text{Nu}_x$ and $\text{Re}_x^{-1/2} \text{Sh}_x$ are referred to as the reduced Nusselt number and reduced Sherwood number denoted by Nu_x and Sh_x , which are represented by $-\theta'(0)$ and $-\phi'(0)$, respectively.

Stability solutions

Rosca and Pop [4], and Weidman *et al.* [10] have shown that the lower branch solutions are unstable (not physically realizable), while the upper branch solutions are stable (physically realizable). Because of the interesting findings mentioned previously, many works on stability analysis have been performed in order to prove the findings which can be found in [28-31]. Firstly, we consider the eqs. (2)-(4) in unsteady form. Thus, we introduce the new dimensionless time variable $\tau = Ut/2x$. The use of τ is associated with an initial value problem and is consistent with the question of which solution will be obtained in practice (physically realizable). Thus, the unsteady eqs. (2)-(4):

$$\frac{\partial u}{\partial t} + u \frac{\partial u}{\partial x} + v \frac{\partial u}{\partial y} = \nu \frac{\partial^2 u}{\partial y^2} \quad (16)$$

$$\frac{\partial T}{\partial t} + u \frac{\partial T}{\partial x} + v \frac{\partial T}{\partial y} = \alpha \nabla^2 T + \Omega \left[D_B \frac{\partial C}{\partial y} \frac{\partial T}{\partial y} + \left(\frac{D_T}{T_\infty} \right) \left(\frac{\partial T}{\partial y} \right)^2 \right] \quad (17)$$

$$\frac{\partial C}{\partial t} + u \frac{\partial C}{\partial x} + v \frac{\partial C}{\partial y} = D_B \frac{\partial^2 C}{\partial y^2} + \left(\frac{D_T}{T_\infty} \right) \frac{\partial^2 T}{\partial y^2} \quad (18)$$

where t denotes the time. We introduce now the following new dimensionless variables:

$$\theta(\eta, \tau) = \frac{T - T_\infty}{T_w - T_\infty}, \quad \phi(\eta, \tau) = \frac{C - C_\infty}{C_w - C_\infty}, \quad \eta = y \sqrt{\frac{U}{2\nu x}}, \quad \psi = (2U\nu x)^{1/2} f(\eta, \tau), \quad \tau = \frac{Ut}{2x} \quad (19)$$

so that eqs. (16)-(18) can be written:

$$\frac{\partial^3 f}{\partial \eta^3} + f \frac{\partial^2 f}{\partial \eta^2} - \frac{\partial^2 f}{\partial \eta \partial \tau} + 2\tau \left(\frac{\partial^2 f}{\partial \eta^2} - \frac{\partial^2 f}{\partial \eta \partial \tau} \right) \frac{\partial f}{\partial \eta} = 0 \quad (20)$$

$$\frac{1}{Pr} \frac{\partial^2 \theta}{\partial \eta^2} + f \frac{\partial \theta}{\partial \eta} + Nb \frac{\partial \theta}{\partial \eta} \frac{\partial \phi}{\partial \eta} + Nt \left(\frac{\partial \theta}{\partial \eta} \right)^2 - 2\tau \frac{\partial f}{\partial \tau} \frac{\partial \theta}{\partial \eta} - \frac{\partial \theta}{\partial \tau} = 0 \quad (21)$$

$$\frac{\partial^2 \phi}{\partial \eta^2} + Le f \frac{\partial \phi}{\partial \eta} + \frac{Nt}{Nb} \frac{\partial^2 \theta}{\partial \eta^2} + Nt \left(\frac{\partial \theta}{\partial \eta} \right)^2 - \frac{\partial \phi}{\partial \tau} - 2\tau \frac{\partial f}{\partial \tau} \frac{\partial \phi}{\partial \eta} = 0 \quad (22)$$

subjected to the boundary conditions:

$$f(0, \tau) = s, \quad \frac{\partial f}{\partial \eta}(0, \tau) = \lambda + \sigma \frac{\partial^2 f}{\partial \eta^2} + \delta \frac{\partial^3 f}{\partial \eta^3}, \quad \theta(0, \tau) = 1, \quad Nb \frac{\partial \phi}{\partial \eta}(0, \tau) + Nt \frac{\partial \theta}{\partial \eta}(0, \tau) = 0$$

$$\frac{\partial f}{\partial \eta}(\eta, \tau) \rightarrow 1, \quad \theta(\eta, \tau) \rightarrow 0, \quad \phi(\eta, \tau) \rightarrow 0, \quad \text{as } \eta \rightarrow \infty \quad (23)$$

To test the stability of the steady flow solution $f(\eta) = f_0(\eta)$, $\theta(\eta) = \theta_0(\eta)$, and $\phi(\eta) = \phi_0(\eta)$ satisfying the boundary value problem eqs. (20)-(23):

$$f(\eta, \tau) = f_0(\eta) + e^{-\gamma \tau} F(\eta), \quad \theta(\eta, \tau) = \theta_0(\eta) + e^{-\gamma \tau} G(\eta), \quad \phi(\eta, \tau) = \phi_0(\eta) + e^{-\gamma \tau} H(\eta) \quad (24)$$

where γ is an unknown eigenvalue, $F(\eta)$, $G(\eta)$, and $H(\eta)$ are small relative to $f_0(\eta)$, $\theta_0(\eta)$, and $\phi_0(\eta)$. Solutions of the eigenvalue problem eqs. (20)-(23) give an infinite set of eigenvalues $\gamma_1 < \gamma_2 < \gamma_3, \dots$. If γ_1 is negative, there is an initial growth of disturbances and the flow is unstable but when γ_1 is positive, there is an initial decay and the flow is stable. Introduce eq. (24) into eqs. (20)-(23), we get the linearized problem:

$$F_0''' + f_0 F_0'' + f_0'' F_0 + \gamma F_0' = 0 \quad (25)$$

$$\frac{1}{Pr} G_0'' + (f_0 + Nb \phi_0' + 2Nt \theta_0') G_0' + \gamma G_0 + Nb \theta_0' H_0' = 0 \quad (26)$$

$$H_0'' + Le f_0 H_0' + Le F_0 \phi_0' + 2 \frac{Nt}{Nb} \theta_0'' G_0'' + \gamma H_0 = 0 \quad (27)$$

along with the boundary conditions:

$$F_0(0) = 0, \quad F_0'(0) = \sigma F_0''(0) + \delta F_0'''(0), \quad G_0(0) = 0, \quad Nb H_0'(0) + Nt G_0'(0) = 0$$

$$F_0'(\eta) \rightarrow 0, \quad G_0(\eta) \rightarrow 0, \quad H_0(\eta) \rightarrow 0 \quad \text{as } \eta \rightarrow \infty \quad (28)$$

It should be stated that for particular values of Nb , Nt , and γ the stability of the corresponding steady flow solutions $f_0(\eta)$, $\theta_0(\eta)$, and $\phi_0(\eta)$ are determined by the smallest eigenvalue γ . As it has been suggested by Harris *et al.* [32], the range of possible eigenvalues can be deter-

mined by relaxing a boundary condition on $F_0(\eta)$, $G_0(\eta)$, or $H_0(\eta)$. For the present problem, we relax the condition that $F'_0(\eta) \rightarrow 0$ as $\eta \rightarrow \infty$, and for a fixed value of σ , δ , Nb , Nt , and Lewis number we solve the system eqs. (25)-(28) along with the new boundary conditions $F''_0 = 1$.

Results and discussion

The ODE (8)-(11) has been solved numerically using code 1 and 2 in *bvp4c* function (MATLAB software) to obtain the missing values, namely $f'''(0)$, $-\theta'(0)$, and $-\phi'(0)$ by guessing a set of initial values until the graphs fulfill the prescribed far field boundary conditions. The similarity variable η at a finite value denoted as η_{\max} and is set to be $\eta_{\max} = 10$ for the first solution while the second solution η_{\max} is set to be $\eta_{\max} = 15$. We run our bulk computations using η_{\max} , which sufficient to satisfy the far field boundary conditions asymptotically for all values of the parameters tested. Our main focus on this study is to test the velocity ratio parameter, λ , when there are slip effects on the flow (first-order slip, σ , and second-order slip, δ). This present study also dealt with nanofluid modeled by Buongiorno [33]. There is some common parameter involved which are Lewis number, Prandtl number, Brownian motion, thermophoresis, and also mass suction.

Table 1 and fig. 2 show the numerical results obtained are in a good agreement with previous works. Variation of skin friction coefficients as well as heat transfer coefficient for various values of σ and δ are illustrate in fig. 3. These figures indicate that skin friction coefficient and heat transfer increased as we increased values of σ and $|\delta|$. The figures also verify that unique solution only occur when $\lambda > 0$, while there exist dual solutions in between $\lambda_c < \lambda < 0$, *i. e.*, when the plate moving upstream (opposite direction) from origin. The solutions exist till the critical value, λ_c (say lambda critical), beyond which the boundary-layer separates from the surface and the solution on boundary-layer approximations are impossible. The values of skin friction coefficient $f'''(0)$ are positive when $\lambda < 1$, while negative values when $\lambda > 1$. Physically, positive sign for $f'''(0)$ implies that the fluid exerts a drag force on the plate and negative sign means opposite way. The variations of heat transfer coefficient $-\theta'(0)$ with λ for several values of Lewis and Prandtl numbers, Nb and Nt are presented in fig. 4. It can be seen that

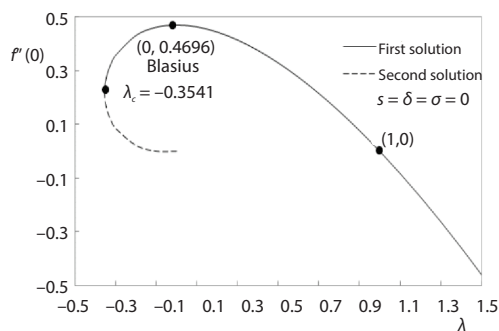


Figure 2. Skin friction coefficient $f'''(0)$ with λ when $s = \sigma = \delta = 0$

the heat transfer coefficient increases as we increased Lewis and Prandtl numbers. However, different observation can be seen that the heat transfer coefficient obviously higher for a nanofluid with smaller values of Nb and Nt . Therefore, with small values of Nb and Nt is sufficient to increase the heat transfer rate at the surface.

Following Fang *et al.* [2], we can point out a further discussion for figs. 5 and 6, which illustrate the effects of the slip parameters σ and δ on the skin friction coefficient as well as heat transfer coefficient as a func-

Table 1. Variation of λ_c for various values of σ and δ

| s | σ | δ | [10] | [24] | Present work |
|-----|----------|----------|---------|---------|--------------|
| 0 | 0 | 0 | -0.3541 | -0.3541 | -0.3541 |
| 1 | 0 | 0 | | | -1.2082 |
| | 0.5 | -0.5 | | | -2.7930 |
| | 1 | -1 | | | -4.5370 |

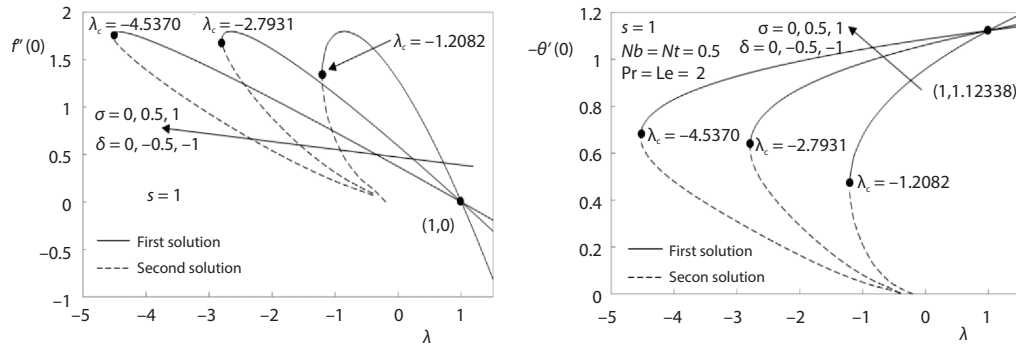


Figure 3. Variation of skin friction coefficient $f''(0)$ and heat transfer coefficient $-\theta'(0)$ with λ for various values of σ and δ

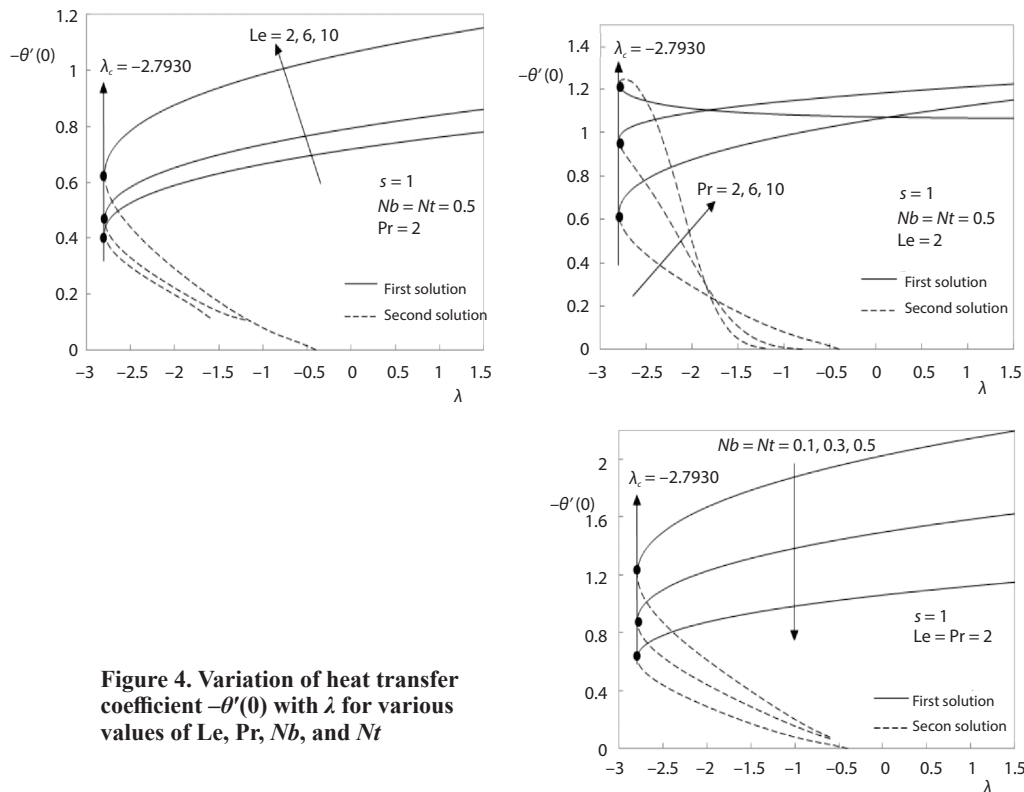


Figure 4. Variation of heat transfer coefficient $-\theta'(0)$ with λ for various values of Le , Pr , Nb , and Nt

tion of moving parameter, λ . As we can see in fig. 5, when only the first order slip parameter, σ , is considered, the skin friction and heat transfer coefficient increased as σ increased. In fig. 6, when only the second order slip parameter, δ , is considered, we choose $s = 2$ because if $s = 1$ the results will be the same as in fig. 6. The skin friction coefficient and heat transfer rate is increasing as $|\delta|$ increases. Addition, the mass suction s is taken into consideration and we presented the graph in fig. 7. Graphically, there exist unique solution when $s > 1.8$, while dual solutions exist up to $s_c < s \leq 1.8$, and no solutions occur $s < s_c$. Figures 8-12

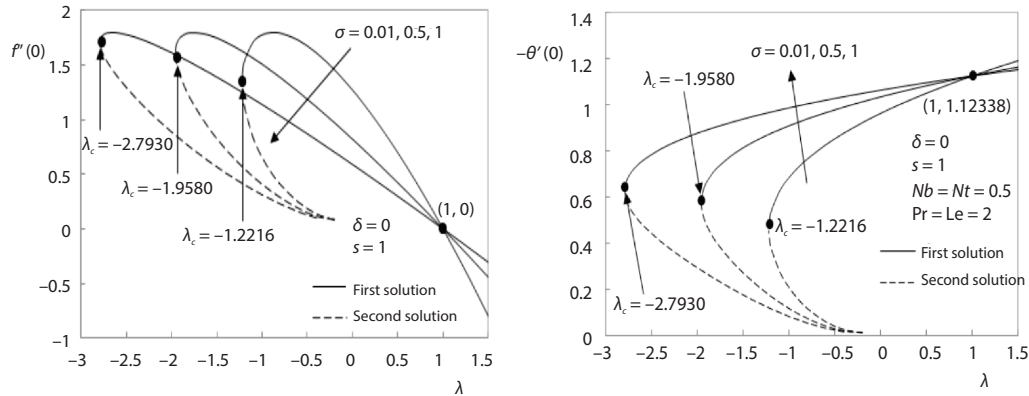


Figure 5. Variation of reduced skin friction coefficient $f''(0)$ and heat transfer coefficient $-\theta'(0)$ with λ for various values of σ

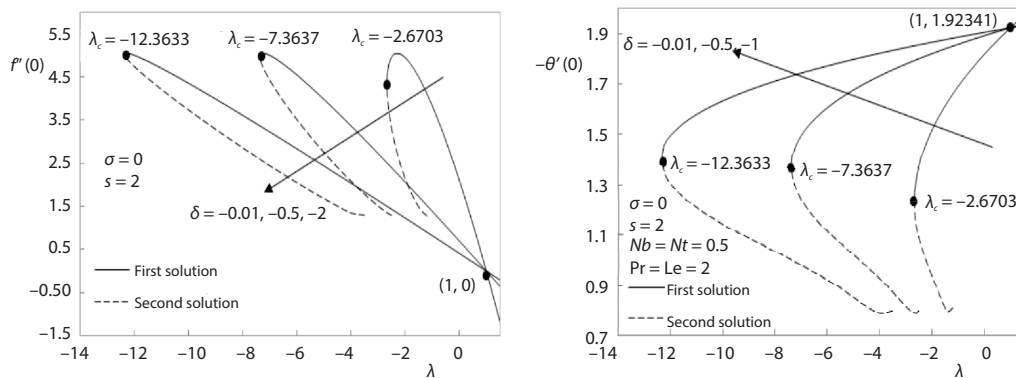


Figure 6. Variation of skin friction coefficient $f''(0)$ and heat transfer coefficient $-\theta'(0)$ with λ for various values of δ

display the velocity, temperature as well as nanoparticle volume fraction profiles for several values of σ , δ , Lewis and Prandtl numbers, and also s . All profiles satisfied the far field boundary conditions eq. (11) asymptotically. From these profiles, we can prove that the dual solutions shown in figs. 1-7 are existed. The boundary-layer thickness for second solution is always thicker than the first solution.

The systems of linear eigenvalue problem eqs. (25)-(28) are then being solved using code 3 and 4 in *bvp4c* function. This type of method is use in order to find the eigenvalues, γ . The computational results were obtained and had been shown in tab. 2. We have comparing our results with those reported by Weidman *et al.* [10] and it is shows that our numerical results are in excellent agreement with previous data. From the table, it is seen that the eigenvalues are approaching 0 when λ is approaching λ_c . The eigenvalues of first solution and second solution will increases as we increased λ . Clearly, the eigenvalues for first solution is positive while the second solution is negative. From the eigenvalues obtained, we can say that the first solution is stable and physically relevant but somehow for the second solution is said to be unstable and not physically relevant.

Table 2. Smallest eigenvalues γ for selected values of λ (moving plate)

| s | σ | δ | λ | [10] | | Present work | |
|---|----------|----------|-----------|----------------|-----------------|----------------|-----------------|
| | | | | First solution | Second solution | First solution | Second solution |
| 0 | 0 | 0 | -0.35 | 0.0576 | -0.0492 | 0.0577 | -0.0492 |
| | | | -0.34 | 0.1134 | -0.0839 | 0.1134 | -0.0839 |
| | | | -0.32 | 0.1879 | -0.1164 | 0.1879 | -0.1164 |
| | | | -0.3 | 0.2470 | -0.1332 | 0.2470 | -0.1332 |
| 1 | 0 | 0 | -1.20 | | | 0.1097 | -0.0963 |
| | | | -1.18 | | | 0.2128 | -0.1669 |
| | | | -1.15 | | | 0.3188 | -0.2240 |
| | | | -1.13 | | | 0.3773 | -0.2499 |
| | 0.5 | -0.5 | -2.79 | | | 0.0431 | -0.0417 |
| | | | -2.5 | | | 0.4677 | -0.3377 |
| | | | -2.3 | | | 0.6240 | -0.4013 |
| | | | -2.1 | | | 0.7554 | -0.4363 |
| | 1 | -1 | -4.53 | | | 0.0501 | -0.0486 |
| | | | -4.5 | | | 0.1168 | -0.1089 |
| | | | -4.3 | | | 0.3083 | -0.2571 |
| | | | -4.1 | | | 0.4279 | -0.3322 |

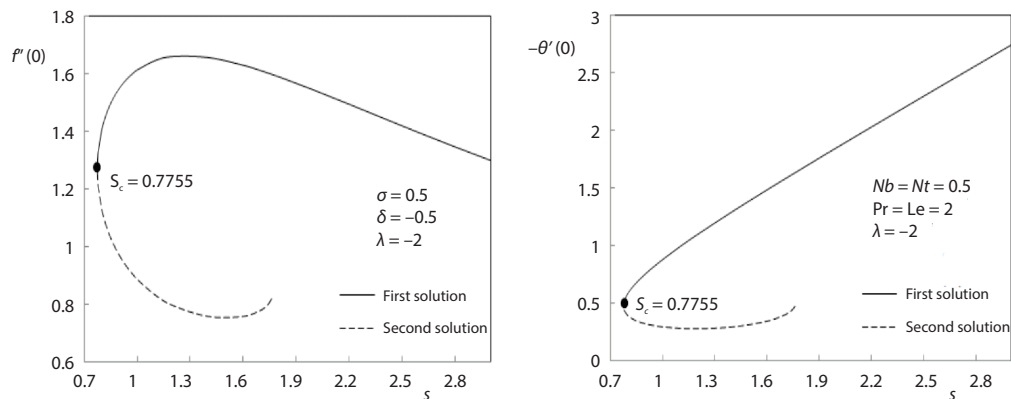


Figure 7. Variation of skin friction coefficient $f''(0)$ and heat transfer coefficient $-\theta'(0)$ with s

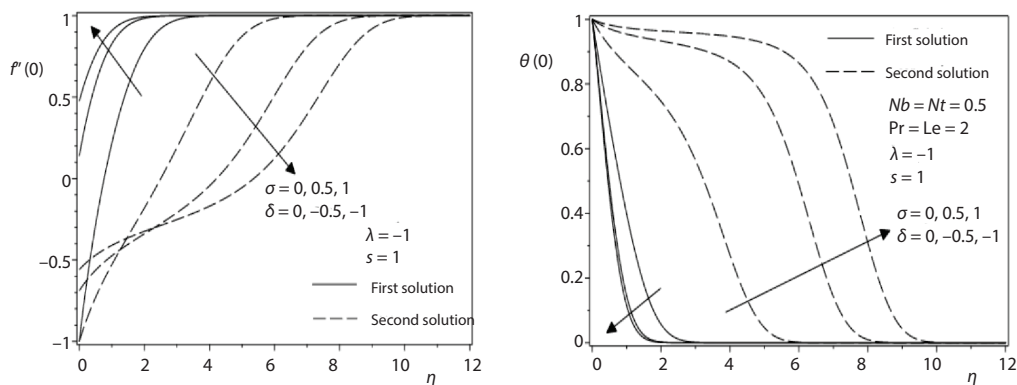


Figure 8. Velocity profiles $f'(\eta)$ and temperature profiles $\theta(\eta)$ for several values of σ and δ

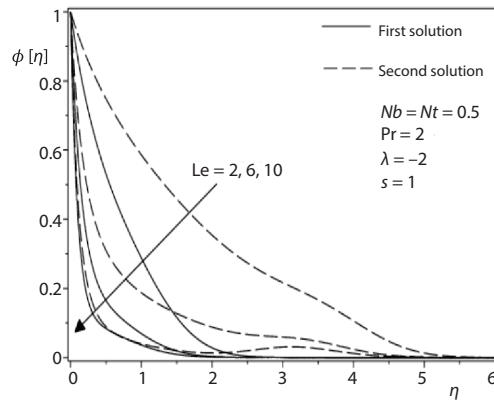


Figure 9. Nanoparticle volume fraction profiles $\phi(\eta)$ for several values of Lewis number

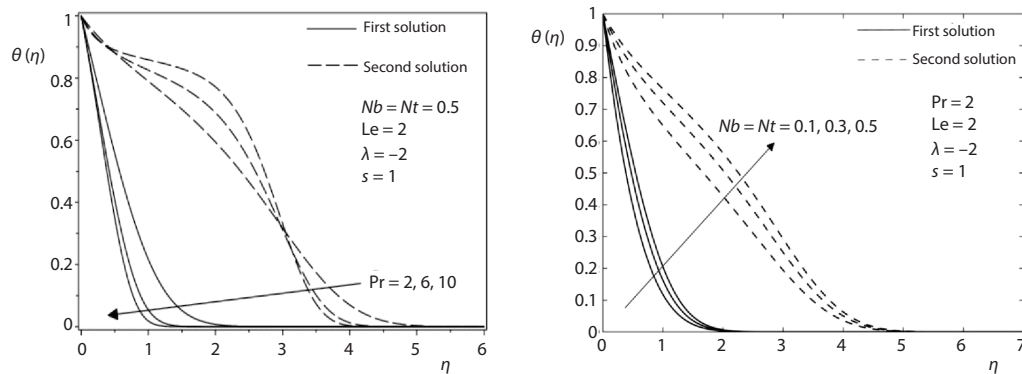


Figure 10. Temperature profiles $\theta(\eta)$ for several values of Pr , Nb , and Nt

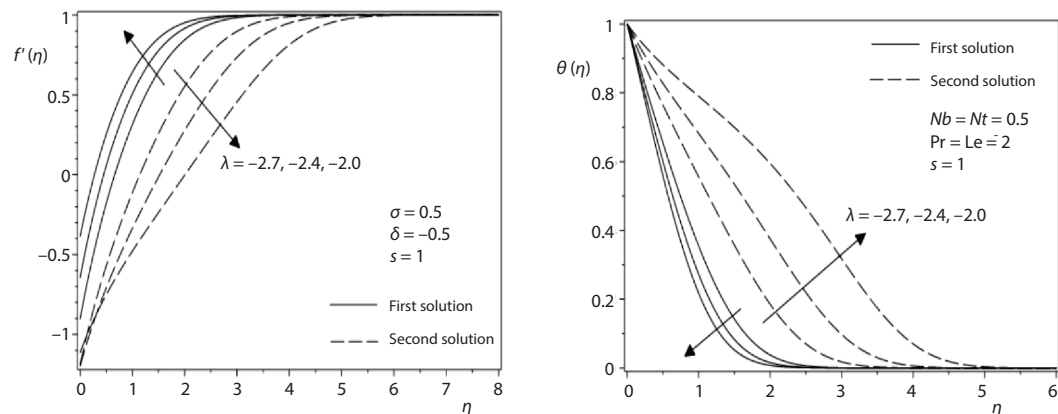


Figure 11. Velocity profiles $f'(\eta)$ and temperature profiles $\theta(\eta)$ for several values of λ

Conclusions

The steady boundary-layer flow of a nanofluid past a moving semi-infinite flat plate in a uniform free stream in the presence of mass suction and second-order slip flow model introduced by Wu [1], and also used by Fang *et al.* [2] and Fang and Aziz [3] is numerically

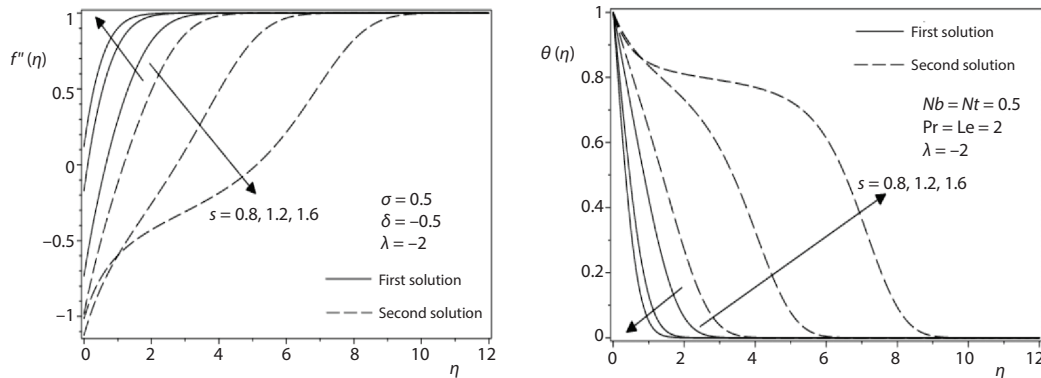


Figure 12. Velocity profiles $f''(\eta)$ and temperature profiles $\theta(\eta)$ for several values of s

studied. The boundary-layer equations in form of PDE are transformed into ODE using appropriate similarity variables before being solved using *bvp4c* function in MATLAB software. The analysis performed that.

- Dual solutions occurred for opposing flow (when the plate and free stream are moving in opposite direction each other), $\lambda < 0$ and in certain range of mass suction up to critical point, $s_c < s \leq 1.8$.
- Largest Lewis and Prandtl numbers are required to enhance the heat transfer coefficient.
- Only small value of Nb and Nt is sufficient to increase the heat transfer coefficient.
- The increment of slip parameters lead to decrease the skin friction coefficient whereas increase the heat transfer coefficient.
- The first solution is linearly stable and physically meaningful, while the second solution is linearly unstable and not physically relevant.

Acknowledgment

We would like to express appreciation the Putra Grant of Universiti Putra Malaysia (Project code: GP-IPS/2016/9513000) in the financial support received.

Nomenclature

A, B – constant
 C – concentration
 C_w – plate concentration
 C_∞ – ambient concentration
 c – volumetric volume expansion coefficient of the nanofluid
 D_B – Brownian diffusion coefficient
 D_T – thermophoretic diffusion coefficient
 Kn – Knudsen number
 k – thermal conductivity
 Le – Lewis number
 Nb – Brownian motion parameter
 Nt – thermophoresis parameter
 Pr – Prandtl number
 Re – Reynolds number
 s – suction

T – temperature
 T_w – plate temperature
 T_∞ – ambient temperature
 t – time
 U – free stream velocity
 U_w – flat plate velocity
 U_{slip} – slip velocity
 u, v – velocity components
 \mathbf{v} – velocity vector
 x, y – co-ordinate system

Greek symbols

α – thermal diffusivity
 δ – second order slip parameter
 λ – moving parameter
 μ – dynamic viscosity

| | | | | | |
|--------------|---|----------|--------------------------------------|--|----------|
| ν | – kinematic viscosity | | | | material |
| ρ | – density | σ | – first order slip parameter | | |
| ρ_f | – density of the base fluid | χ | – momentum accommodation coefficient | | |
| ρ_p | – density of the particles | ω | – the molecular mean free path | | |
| $(\rho c)_f$ | – heat capacity of the fluid | | | | |
| $(\rho c)_p$ | – effective heat capacity of the nanoparticle | | | | |

References

- [1] Wu, L., A Slip Model for Rarefied Gas-Flows at Arbitrary Knudsen Number, *Applied Physics Letter*, 93 (2008), ID 253103
- [2] Fang, T., *et al.*, Viscous Flow over a Shrinking Sheet with a Second-Order Slip Flow Model, *Comm. Non-Linear Sci Numer Simulat*, 15 (2010), 7, pp. 1831-1842
- [3] Fang, T., Aziz, A., Viscous Flow with Second-Order Slip Velocity over a Stretching Sheet, *Z. Naturforsch. A*, 65 (2010), 12, pp. 1087-1092
- [4] Rosca, A.V., Pop, I., Flow and Heat Transfer over a Vertical Permeable Stretching/Shrinking Sheet with a Second order Slip, *International Journal of Heat and Mass Transfer*, 60 (2013), May, pp. 355-364
- [5] Rosca, N. C., Pop, I., Mixed Convection Stagnation Point Flow Past a Vertical Flat Plate with a Second Order Slip: Heat Flux Case, *International Journal of Heat and Mass Transfer*, 65 (2013), Oct., pp. 102-109
- [6] Mabood, F., Das, K., Melting Heat Transfer on Hydromagnetic-Flow of a Nanofluid over a Stretching Sheet with Radiation and Second Order Slip, *The European Physical Journal Plus*, 131 (2016), 1, pp. 1-31
- [7] Wu, L., Mass Transfer Induced Slip Effect on Viscous Gas-Flows above a Shrinking/Stretching Sheet, *International Journal of Heat and Mass Transfer*, 93 (2016), Feb., pp. 17-22
- [8] Sharma, R., Ishak, A., Second order Slip Flow of Cu-Water Nanofluid over a Stretching Sheet with Heat Transfer, *WSEAS Transaction on Fluid Mechanics*, 9 (2014), Jan., pp. 26-33
- [9] Merkin, J. H., On Dual Solutions Occuring in Mixed Convection in a Porous Medium, *Journal of Engineering Mathematics*, 20 (1985), June, pp. 171-179
- [10] Weidman, P. D., *et al.*, The Effects of Transpiration on Self-Similar Boundary-Layer Flow over Moving Surfaces, *International Journal of Engineering Sciences*, 44 (2006), 11-12, pp. 730-737
- [11] Merrill, K., *et al.*, Final Steady Flow Near a Stagnation Point on a Vertical Surface in a Porous Medium, *International Journal of Heat and Mass Transfer*, 49 (2006), 23-24, pp. 4681-4686
- [12] Ishak, A., Flow and Heat Transfer over a Shrinking Sheet: A Stability Analysis, *International Journal of Mechanical, Aerospace, Industrial and Mechatronics Engineering*, 8 (2014), 5, pp. 905-909
- [13] Noor, A., *et al.*, Stability Analysis of Stagnation-Point Flow Past a Shrinking Sheet in a Nanofluid, *Journal of Quality Measurement and Analysis*, 10 (2014), 2, pp. 51-63
- [14] Nazar, R., *et al.*, Stability Analysis of 3-D Flow and Heat Transfer over a Permeable Shrinking Surface in a Cu-Water Nanofluid, *International Journal of Mathematical, Computational, Physical, Electrical and Computer Engineering*, 8 (2014), 5, pp. 782-788
- [15] Noor, A., *et al.*, Stability Analysis of Flow and Heat Transfer on a Permeable Moving Plate in a Co-Flowing Nanofluid, *Proceedings, The 2014 UKM FST Postgraduate Colloquium*, Selangor, Malaysia, 2014, Vol. 1614, pp. 898-905
- [16] Hafidzuddin, E. H., *et al.*, Stability Analysis of Unsteady 3-D Viscous Flow over a Permeable Stretching/Shrinking Surface, *Journal of Quality Measurement and Analysis*, 11 (2015), 1, pp. 19-31
- [17] Yasin, M. H. M., *et al.*, The MHD Stagnation-Point Flow and Heat Transfer with Effects of Viscous Dissipation, Joule Heating and Partial Velocity Slip, *Scientific Reports*, 5 (2015), ID17848
- [18] Blasius, H., Boundary Layers in Liquids with Low (in German), *Journal Math. Phys.*, 56 (1908), pp. 1-37
- [19] Klemp, J. P., Acrivos, A., A Moving-Wall Boundary-Layer with Reverse Flow, *Journal of Fluid Mechanics*, 53 (1972), 1, pp. 177-191
- [20] Husaini, M. Y., *et al.*, On Similarity Solution of a Boundary-Layer Problem with Upstream Moving Wall, *SIAM Journal of Applied Mathematics*, 7 (1987), 4, pp. 699-709
- [21] Fang, T., Similarity Solutions for a Moving-Flat Plate Thermal Boundary Layer, *Acta Mechanica*, 163 (2003), 3-4, pp. 161-172
- [22] Fang T., Further Study on a Moving-Wall Boundary-Layer Problem with Mass Transfer, *Acta Mechanica*, 163 (2003), 3-4, pp. 183-188

- [23] Fang, T., Lee, C. F., A Moving-Wall Boundary-Layer Flow of a Slightly Rarefied Gas Free Stream over a Moving Flat Plate, *Applied Mathematics Letters*, 18 (2005), 5, pp. 487-495
- [24] Bachok, N., et al., Boundary-Layer Flow of Nanofluids over a Moving Surface in a Flowing Fluid, *International Journal of Thermal Sciences*, 49 (2010), 9, pp. 1663-1668
- [25] Kuznetsov, A. V., Nield, D. A., Natural Convective Boundary-Layer Flow of a Nanofluid Past a Vertical Plate, *International Journal of Thermal Sciences*, 49 (2010), 2, pp. 243-247
- [26] Kuznetsov, A. V., Nield, D. A., The Cheng-Minkowycz Problem for Natural Convective Boundary-Layer Flow in a Porous Medium Saturated by a Nanofluid: A Revised Model, *International Journal of Heat and Mass Transfer*, 65 (2013), Oct., pp. 682-685
- [27] Mukhopadhyay, S., Andersson, H. I., Effects of Slip and Heat Transfer Analysis of Flow over an Unsteady Stretching Surface, *Heat Mass Transfer*, 45 (2009), 11, pp. 1447-1452
- [28] Dzulkifli, N. F., et al., Soret and Dufour Effects on Unsteady Boundary-Layer Flow and Heat Transfer of Nanofluid over a Stretching/Shrinking Sheet: A Stability Analysis, *Journal of Chemical Engineering and Process Technology*, 8 (2017), 3, ID1000336
- [29] Bakar, S. A., et al., A Stability Analysis on Mixed Convection Boundary-Layer Flow Along a Permeable Vertical Cylinder in a Porous Medium Filled with a Nanofluid and Thermal Radiation, *Applied Sciences*, 8 (2018), ID483
- [30] Najib, N., et al., Stability Analysis of Stagnation-Point Flow in a Nanofluid over a Stretching/Shrinking Sheet with Second-Order Slip, Soret and Dufour Effects: A Revised Model, *Applied Sciences*, 8 (2018), ID 642
- [31] Bakar, N. A. A., et al., Stability Analysis on the Flow and Heat Transfer of Nanofluid Past a Stretching/Shrinking Cylinder with Suction Effect, *Results in Physics*, 9 (2018), June, pp. 1335-1344
- [32] Harris, S. D., et al., Mixed Convection Boundary-Layer Flow Near the Stagnation Point on a Vertical Surface in a Porous Medium: Brinkman Model with Slip, *Transport Porous Media*, 77 (2009), Dec., pp. 267-285
- [33] Buongiorno, J., Convective Transport in Nanofluids, *ASME J. Heat Transfer*, 128 (2006), 3, pp. 240-250